Liquid Crystals

Publication details, including instructions for authors and subscription information:
http://www.informaworld.com/smpp/title~content=t713926090

Unusual phase behaviour of a new liquid-crystalline side group polymer

D. Wolff[a]; H. Cackovic[b]; H. Krüger[c]; J. Rübner[a]; J. Springer[b]
[a] Projektgruppe im WIP, Berlin, Germany [b] Institut für Technische Chemie, Technische Universität Berlin, Berlin 12, Germany [c] Fraunhofer-Institut für Angewandte Materialforschung, Außenstelle Teltow, Tetlow-Seehof, Germany

To cite this Article Wolff, D. , Cackovic, H. , Krüger, H. , Rübner, J. and Springer, J.(1993) 'Unusual phase behaviour of a new liquid-crystalline side group polymer', Liquid Crystals, 14: 3, 917 — 928

To link to this Article: DOI: 10.1080/02678299308027769

URL: http://dx.doi.org/10.1080/02678299308027769

LIQUID CRYSTALS, 1993, VOL. 14, NO. 3, 917–928

Unusual phase behaviour of a new liquid-crystalline side group polymer

by D. WOLFF†, H. CACKOVIC‡, H. KRÜGER§,
J. RÜBNER† and J. SPRINGER‡*

† Projektgruppe im WIP, Rudower Chaussee 5, O-1199 Berlin, Germany
‡ Institut für Technische Chemie, Technische Universität Berlin,
W-1000 Berlin 12, Germany
§ Fraunhofer-Institut für Angewandte Materialforschung,
Außenstelle Teltow, Kantstr. 55, O-1530 Tetlow-Seehof, Germany

The phase structure of a series of liquid-crystalline side group polymethacrylates with azo-groups in the mesogenic units was investigated by X-ray diffraction and differential scanning calorimetry. The influence of the spacer and tail length on the nature of the liquid crystal phase is discussed. For one polymer, depending on the annealing temperature, a phase transition from a metastable monolayer S_A phase to a bilayer S_C phase and to an unidentified phase, possibly crystalline, was found. This behaviour is discussed considering steric hindrance of the mesogenic side groups and the anisotropic conformation of the backbone.

1. Introduction

The interest in synthesis and structural investigations of side group liquid-crystalline polymers with azo-groups in the mesogenic units has increased due to their potential application in the field of non-linear optics, in optical storage and in electro-optical displays [1–7]. The photo-responsive azobenzene group appears particularly interesting because irradiation can cause the *trans→cis* isomerization of the photochromic group, so inducing a local phase transition [8–13]. Additionally, the azo-containing mesogenic group may act as a convenient photo-responsive probe of polymer conformation, both in bulk and in solution [14].

Here we describe the phase structure of a series of side group liquid-crystals (for the polymer general structure see figure 1) investigated by X-ray diffraction and differential scanning calorimetry. Because of the relative rigidity of the methacrylate backbone, it was of great interest to study the formation of smectic layers, assuming steric hindrance of the side groups if the spacer and the tail groups have nearly the same lengths.

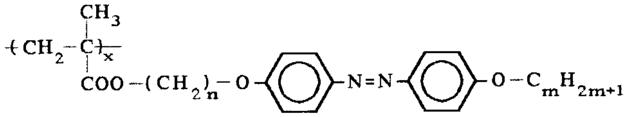

Figure 1. Investigated polymers $P_{n,m}$: $P_{6,2}$, $P_{6,4}$, $P_{6,6}$, $P_{4,4}$ and $P_{8,4}$.

---

* Author for correspondence.

0267–8292/93 $10·00 © 1993 Taylor & Francis Ltd.

2. Experimental

2.1. *Synthesis*

The polymethacrylates with spacer-linked 4-alkoxy-azobenzene moieties were synthesized from the alkoxyanilines **1** (see the scheme). By diazotization and coupling on to phenol, the azobenzene chromophore **2** was obtained. The azobenzene **2** and a ten-fold excess of an α,ω-dibromoalkane gave the 4-*n*-alkoxy-4′-ω-bromo-alkoxyazobenzene **3**. The monomer **4** was synthesized by interaction of **3** with the potassium salt of methacrylic acid in dimethylformamide.

For diazotization, the 4-alkoxyanilines **1** with $m = 2$ and 6 were used as supplied by Aldrich without further purification. The alkoxyanilines **1** with $m = 3$, 4 and 5 were synthesized from 4-acetamidophenol as shown in the scheme for 4-butoxyaniline.

0·497 mol of 4-acetamidophenol were mixed with stirring with a solution of 27 g of potassium hydroxide in 750 ml of aqueous ethanol (50 wt%). Then 72·6 g of butyl bromide in 750 ml of butan-p-ol were added and the solution was vigorously stirred

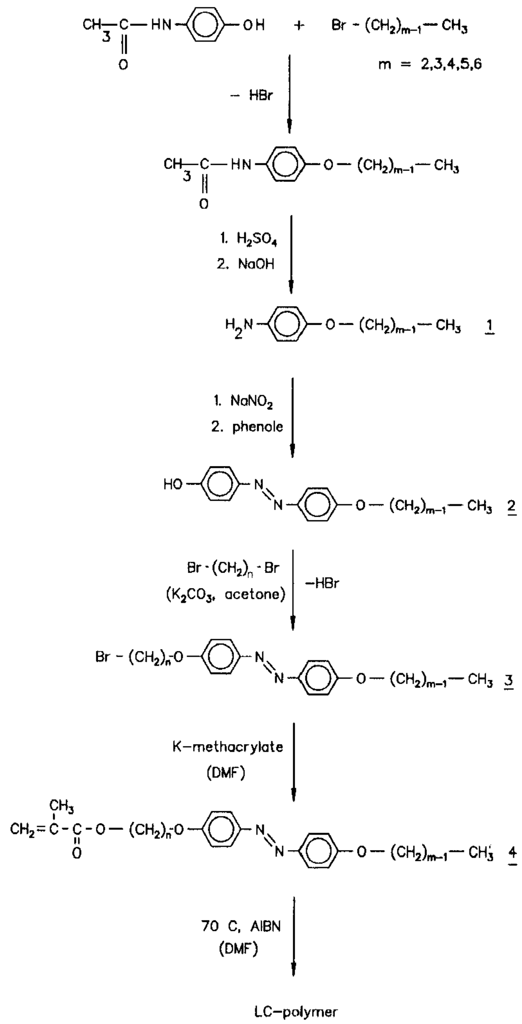

Scheme. Synthetic route.

under reflux for 12 h. Most of the solvent was removed by rotary evaporation. The precipitate was filtered off and washed with 5 per cent aqueous NaOH and with water. The product was heated with 398 ml of sulphuric acid (20 wt%) at 95°C for 1·5 h. Then the solution was cooled to room temperature. The precipitate was filtered off and washed with water.

The amine salt was suspended in 750 ml water at 80°C and a solution of 15 g of NaOH in 30 ml of water was added until the mixture was alkaline. The crude aniline liberated was extracted (twice) into diethyl ether. The ether phase was dried over sodium hydroxide and the ether evaporated. The dark liquid was fractionated by vacuum distillation at 50 Pa, yielding 35 g of pure 4-butoxyaniline (purity checked by GC >99·6 per cent).

4-Butoxy-4'-hydroxy-azobenzene **2** ($m=4$) was obtained by diazotization of 4-butoxyaniline (0·2 mol) in 50 per cent, v/v hydrochloric acid (90 ml). The solution was cooled to 5°C and 10·1 g of sodium nitrite in 58 ml of water was added dropwise keeping the temperature below 5°C. The diazonium salt solution was added in small portions at a temperature of 5°C to a solution of 41 g of phenol dissolved in a solution of 34·8 g of NaOH in 430 ml of water. The precipitated azo dye, after addition of sodium chloride, was filtered off and washed with ice water and dried. The dye was purified by multiple recrystallizations from ethanol/water. The yield was 50 per cent. The other azo dyes **2** were synthesized similarly.

Compounds **3** were obtained as exemplified for 4-(6-bromohexyloxy)-4'-butyloxyazobenzene **3** ($n=6, m=4$). 5·4 g (0·02 mol) of 4-butoxy-4'-hydroxyazobenzene were dissolved in 200 ml of dry acetone; 0·2 mol of 1,6-dibromohexane, 14 g of dry potassium carbonate, 0·3 g of potassium iodide and 50 ml of dry acetone were added and the mixture heated under reflux. The mixture was cooled to room temperature, and the precipitate filtered off and washed with small amounts of acetone and water. The filtrate was almost completely evaporated to dryness and the precipitate washed in the same way as described above. The combined yellow products were recrystallized several times from ethanol/toluene. The yields for all the compounds **3** were between 49·4 and 83·5 per cent.

The monomers **4** were obtained as now described for 4-ω-methacryloyloxy-hexyloxy-4'-butoxyazobenzene **4** ($n=6, m=4$). 0·01 mol of potassium methacrylate and 0·005 mol of 4-(6-bromohexyloxy)-4'-butoxyazobenzene **3** ($n=6$, $m=4$) were added to 70 ml of dimethylformamide and heated under nitrogen atmosphere at 60°C for 10 h. The reaction mixture was cooled to room temperature and poured into 200 ml of water. The yellow crystals were filtered off and were nearly pure. Recrystallization was however carried out from ethanol/toluene. Elemental analysis data for the monomers are given in table 1.

Table 1. Elemental analysis data for the monomers (calculated values in parenthesis).

Monomer	C/%	H/%	N/%
$M_{6,2}$	70·34 (70·22)	7·50 (7·37)	6·79 (6·82)
$M_{6,6}$	72·08 (72·07)	8·30 (8·21)	5·95 (6·00)
$M_{4,4}$	69·81 (70·22)	7·48 (7·37)	6·63 (6·82)
$M_{6,4}$	71·93 (71·33)	8·00 (7·76)	6·55 (6·39)
$M_{8,4}$	72·04 (72·07)	8·27 (8·21)	5·98 (6·00)

The polymerizations were carried out using solutions in dimethylformamide at 70°C. As initiator azobisisobutyronitrile was used. The polymerizations were stopped after 24 h and the polymers were purified by multiple reprecipitation from tetrahydrofuran/ethanol–hexane.

2. Measurements

$\bar{M}_w$ values and polydispersity indices, $\bar{M}_w/\bar{M}_n$, for the polymers were determined by gel permeation chromatography (GPC) using polystyrene as standard (ultrastyragel columns from Polymer Labs Ltd., tetrahydrofuran as eluent). Additional small angle light scattering measurements were carried out using a KMX-6 apparatus (Fa. Chromatix).

The phase transition temperatures for the polymers were determined by differential scanning calorimetry using a Perkin–Elmer DSC 7 apparatus at a scanning rate of 10 K min^{-1}. Indium was used for calibration. The maxima of the DSC enthalpy peaks were taken as the phase transition temperatures. For each annealing experiment the polymer samples (4–8 mg) were heated above their clearing temperatures (max. of 170°C in order to prevent thermal degradation). Then the samples were cooled to the annealing temperature at a rate of 10 K min^{-1}. After annealing and fast cooling to room temperature, DSC curves were recorded using a heating rate of 10 K min^{-1}.

The X-ray investigations on oriented samples were carried out using a home made temperature controlled ($\Delta T = \pm 0{\cdot}1$ K) vacuum chamber with a flat film camera at a distance of 81·5 mm from the sample. Monochormatic Cu–K$_\alpha$ radiation ($\lambda = 0{\cdot}15418$ nm, graphite monochromator) was focused by a glass capillary. The polymer samples were oriented inside the chamber in a magnetic field (2·4 T) perpendicular to the incident beam. The samples were heated above their clearing temperatures and cooled to the measuring temperature at a rate of 0·1 K h^{-1}. In the case of polymer $P_{6,4}$, the samples were oriented in the nematic phase and then rapidly cooled to the measuring temperature. Unoriented powder samples were investigated with a horizontal Guinier goniometer (Fa. Siemens).

3. Results and discussion

The phase transition temperatures of the polymers $P_{n,m}$ (for the general structure see figure 1) obtained by differential scanning calorimetry and the phase assignments according to the X-ray investigations on magnetically aligned samples are summarized in table 2. In the case of smectic phases, the measured layer spacings and the calculated side group lengths assuming an all-*trans* conformation of the spacer and tail groups are listed in table 3. As expected there is a decrease in the clearing temperatures with increasing numbers of methylene groups in both the spacer and the tail.

The more closely the ratio of spacer length to length of tail is to 1, the higher is the probability of finding only smectic phases. For instance, the ranges of the nematic phases of polymers $P_{6,2}$ and $P_{8,4}$ were 55° and 13°, respectively, whereas only smectic phases could be observed for polymer $P_{6,6}$ and polymer $P_{4,4}$. If the difference between spacer length and tail length is larger than one methylene group ($P_{6,2}$; $P_{8,4}$), then between the glass transition and the nematic phase only smectic A phases with layer spacings comparable with the length of a single mesogenic unit were found (for $P_{8,4}$, an additional short range S_B phase with the same layer spacing as the S_A phase was present).

Table 2. Weight average molecular weights, polydispersity indices and liquid crystal phase assignments for the polymers $P_{n,m}$.

Polymer	$\bar{M}_w$/g mol^{-1}†	$\bar{M}_w/\bar{M}_n$	Phase transition behaviour/°C								
$P_{6,2}$	74000	1·9	g	70			S_{A_1}	97	N	152	I
$P_{6,6}$	21000	1·5	g	n.d.			S_{C_2}	120	S_{A_d}	140	I
$P_{4,4}$	38000	1·5	g	n.d.			S_{C_2}	143	S_{A_d}	148	I
$P_{8,4}$	62000	2·0	g	84	S_B	89	S_{A_1}	130	N	143	I
$P_{6,4,a}$	39000	1·7	g	93	X	98	$S_{A_1,m}$	116	N	141	I
$P_{6,4,b}$§	53000	1·4	g	96	X	102	$S_{A_1,m}$	119	N	144	I
			g	n.d.			S_{C_2}	133	N	144	I
$P_{6,4,c}$	131000 167000‡	2·3	g	96	X	103	$S_{A_1,m}$	121	N	146	I

† GPC/PS standard; ‡ light scattering; § 3 h annealed at 115°C.

S_{A_1}, smectic A phase, layer spacing: single side group length; $S_{A_1,m}$, metastable S_{A_1} phase; S_{A_d}, smectic A phase: layer spacing between the length of a single and a double side group length; S_{C_2}, smectic C phase: layer spacing is double the length of the side group; g, glass phase; N, nematic phase; S_B, smectic B phase; X, unidentified phase (crystalline?); n.d., not determined, glass transition is broadened.

Table 3. Collected layer spacings from the X-ray patterns of polymers $P_{n,m}$ oriented in a magnetic field and calculated side group lengths assuming an all-*trans* conformation.

Polymer	Calculated side group length/nm	Liquid crystal phase	Layer spacing/nm	Tilt angle/°	Resulting side group length/nm
$P_{6,2}$	2·49	S_{A_1}	2·62	—	
$P_{6,6}$	2·99	S_{A_d}	4·60	—	
		S_{C_2}	4·49	36	2·77
$P_{4,4}$	2·49	S_{A_d}	3·95	—	
		S_{C_2}	3·87	34	2·33
$P_{8,4}$	2·99	S_{A_1}	3·25	—	
$P_{6,4}$	2·75	$S_{A_1,m}$	2·95	—	
		S_{C_2}	4·02	45	2·84

For polymers with the same spacer and tail length ($P_{4,4}$; $P_{6,6}$), a quite different phase behaviour was observed. Below the clearing temperature, a smectic A phase with a layer spacing between a single and double side group length (S_{Ad}) was found. Below the S_{A_d} phase, for both polymers, a smectic C phase with a layer spacing comparable with double the side group length (S_{C2}) was detected (see table 2). Because the glass transitions of these polymers are very broad, the glass transition temperatures were not determined.

Comparing these results, it was of great interest to see which phase behaviour would be observed for a polymer with nearly the same spacer and tail lengths (polymer $P_{6,4}$), considering the steric hindrance of the spacer and tail groups. Independent of the molecular weight for this polymer, below a nematic phase a metastable S_{A_1} phase was found [15]. Just above the glass transition, a further phase transition was detectable using DSC. The transition temperatures and phase assignments are given in table 1. The X-ray patterns of samples of polymer $P_{6,4,b}$ oriented in a magnetic field perpendicular to the incident beam are shown in figure 2. After annealing in the nematic phase the samples were cooled very quickly to obtain the three different phases.

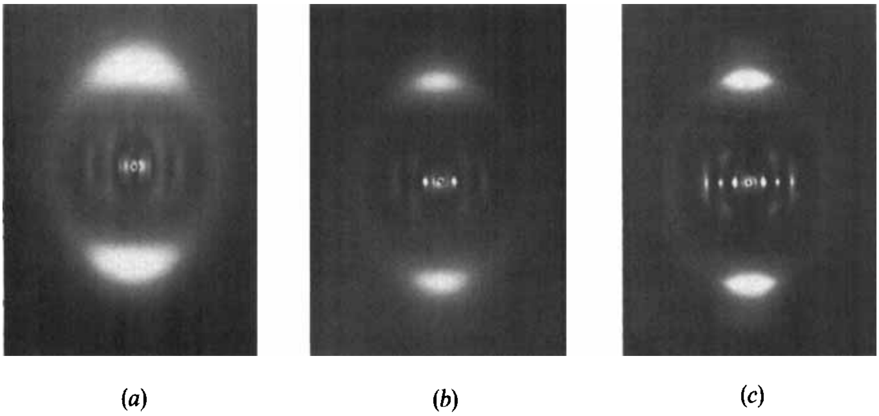
(*a*) (*b*) (*c*)

Figure 2. X-ray patterns of oriented samples of polymer $P_{6,4,b}$; magnetic field direction horizontal. (*a*) Nematic phase at 130°C; exposure time 10 h. (*b*) Metastable S_{A_1} phase after orientation of the nematic phase and rapid cooling to 108°C; exposure time 5 h. (*c*) Unidentified phase after orientation of the nematic phase and rapid cooling to 102°C; exposure time 5 h.

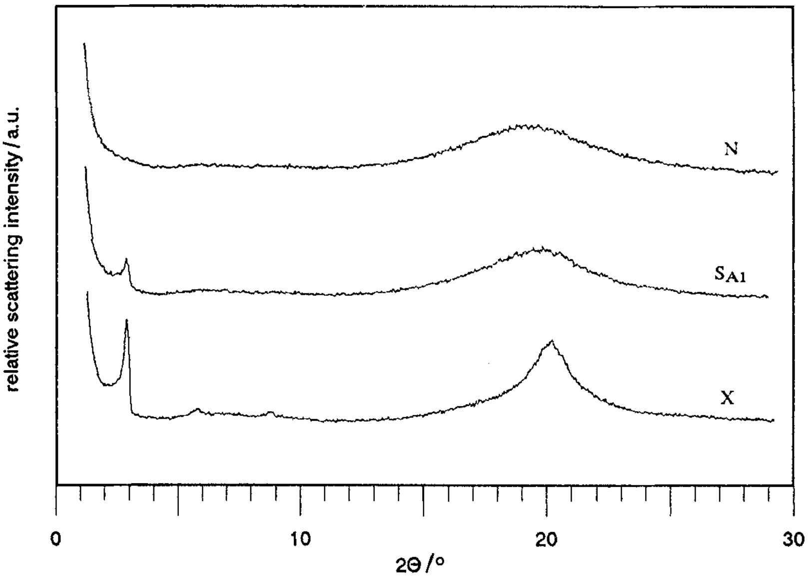

Figure 3. Guinier goniometer curves for polymer $P_{6,4,b}$ (unoriented, not annealed). N, nematic phase at 130°C; S_{A_1}, metastable S_{A_1} phase at 108°C; X, unidentified phase at 102°C.

The corresponding X-ray diffractograms of the nematic phase, the metastable S_{A_1} phase and the unidentified phase (X) just above the glass transition of samples of unoriented polymer $P_{6,4,b}$ are given in figure 3. The observed phase behaviour (glass ↔X↔metastable S_{A_1}↔N) is very similar to that of the polymers having a different spacer and tail length ($P_{6,2}$; $P_{8,4}$). However, on annealing in the metastable S_{A_1} phase, two stable phases depending on the annealing temperature are observed independent of the molecular weight of the polymer. In the following, this behaviour is discussed for polymer $P_{6,4,b}$. After cooling the sample from the isotropic phase to a given temperature between 123°C and 80°C, annealing it for 3 h, and cooling it to room temperature, a DSC heating run was analysed. In figure 4 (*a*) some of these DSC traces are shown. Considering the transition enthalpies (figure 4 (*b*)) and the corresponding transition temperatures (see figure 4 (*c*)), it is possible to distinguish three different processes. On annealing at certain temperatures between 121°C (onset of N→metastable S_{A_1} transition) and 104°C the S_{A_1} phase will be transformed into a S_{C_2} phase. Annealing below 104°C, the transition to the S_{C_2} phase does not occur and a transition from S_{A_1} to a monolayered X phase is observed. At temperatures below 100°C, this transition is marked by processes due to thermal ageing. Investigation of the S_{A_1}→S_{C_2} phase transition by X-ray diffraction techniques was possible depending on annealing time; at 109°C, the transition was slow enough to detect both in

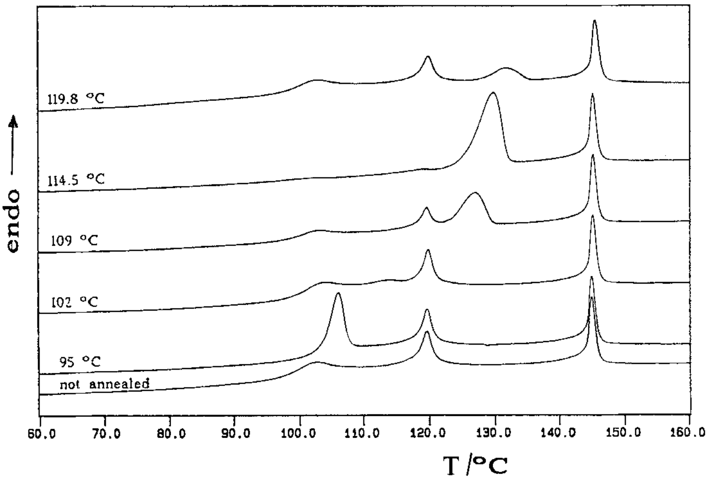

(*a*)

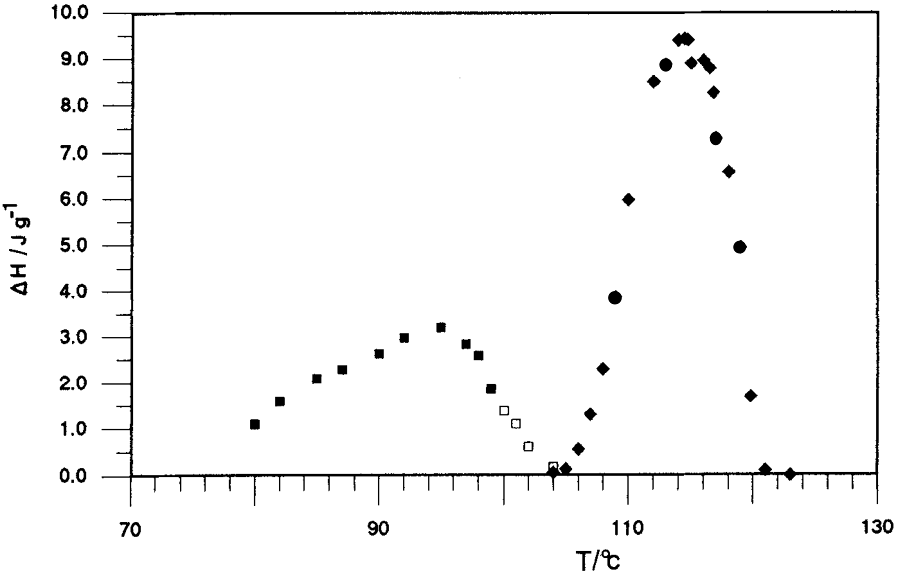

(*b*)

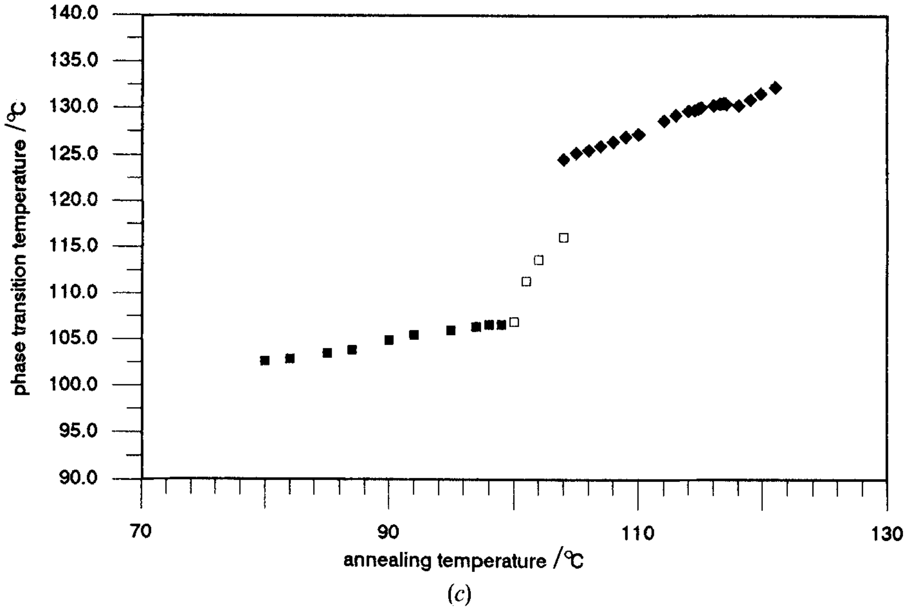

(*c*)

Figure 4. (*a*) DSC traces of polymer $P_{6,4,b}$ depending on annealing temperature; annealing time: 3 h. (*b*) Enthalpies of the phase transitions of polymer $P_{6,4,b}$ observed after annealing (3 h) at different temperatures. (*c*) Transition temperatures for the phases of polymer $P_{6,4,b}$ observed after annealing (3 h) at different temperatures. ■, Ageing and X—S_A transition; □, X–S_A transition; ◆, S_C–N transition.

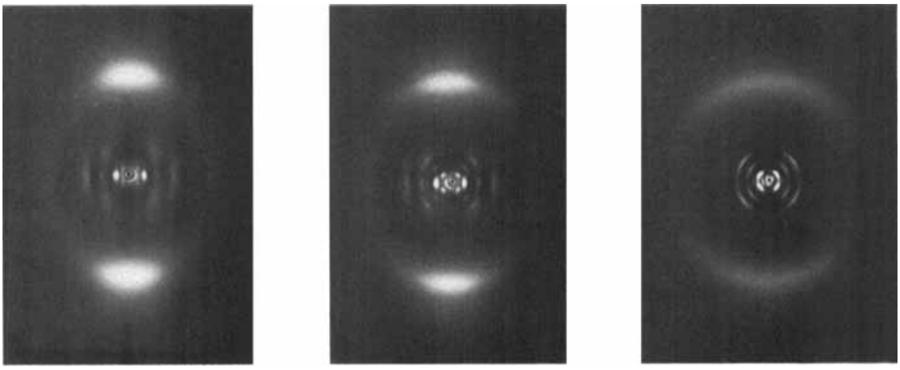

(*a*) (*b*) (*c*)

Figure 5. X-ray patterns of oriented samples of polymer $P_{6,4,b}$ depending on annealing time at 109°C; magnetic field direction horizontal. (*a*) After 12 h; exposure time 5 h. (*b*) After 24 h; exposure time 5 h. (*c*) After 100 h; exposure time 5 h.

magnetically oriented (see figures 5 (*a*)–(*c*)) and powder samples (see figure 6). While in the small angle region, corresponding to the layer spacings, a change in the position and the intensity of the Bragg reflections could be observed, no splitting of the wide angle diffuse crescent was found. Therefore no evidence for a crystallization process could be determined. Because of three orders of Bragg reflections in the S_{C_2} phase, in corresponding domains the layers must be better ordered than in the metastable S_{A_1} phase (only a first order of Bragg reflection was detected).

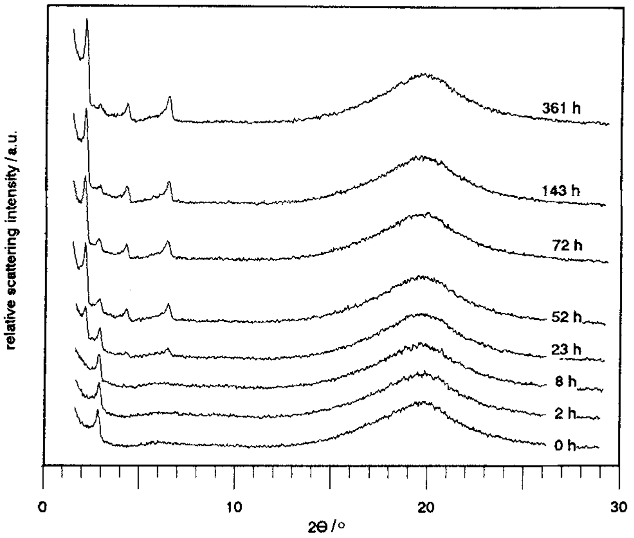

Figure 6. Guinier goniometer curves for polymer $P_{6,4,b}$ depending on annealing time at 109°C.

It was possible to study the kinetics of the $S_{A_1} \rightarrow S_{C_2}$ transition depending on annealing time at 115°C by observing the $S_{C_2} \rightarrow N$ phase transition by DSC after annealing (see figures 7 (*a*) and (*b*)). Figure 7 (*a*) shows some corresponding DSC heating traces. The enthalpies of the $S_{C_2} \rightarrow N$ phase transition are displayed in figure 7 (*b*). Annealing between 1 and 2·5 h at this temperature, we conclude that a linear decrease in S_{A_1} domain size and an increase in S_{C_2} domain size occurs. Annealing at 104°C, both the phase transition from the metastable S_{A_1} to the unidentified X phase and the phase transition from the metastable S_{A_1} to the S_{C_2} phase were observed by DSC. In figure 8 some DSC traces recorded after different annealing times are shown. For instance, during an annealing of 18 h at 104°C, most of the metastable S_{A_1} domains undergo a transition to the phase assigned as X, while some metastable S_{A_1} domains are able to undergo a transition to the S_{C_2} phase. This can be concluded by analysing the enthalpies of the two different DSC peaks resulting on annealing. After annealing at 103°C and recording the corresponding X-ray diffractogram of an unoriented sample (see figure 9), it is supposed that the unidentified phase (X) could be a crystalline phase. Further investigations on magnetically oriented samples are in progress.

4. Conclusions

A decrease in the clearing temperatures with increasing numbers of methylene groups in both the spacer and the tail was found. The closer the ratio of the spacer length to the length of the tail is to 1, the higher is the probability of finding only smectic phases. For such polymers ($P_{4,4}$; $P_{6,6}$) tilted phases were also found (after annealing also for $P_{6,4}$). For sample $P_{6,4}$, depending on annealing temperature, phase transitions were found from a metastable monolayer S_{A_1} phase to a stable bilayer S_{C_2} phase and from the metastable monolayer S_{A_1} phase to an unidentified phase (crystalline?) with Bragg spots that indicate that it too has a monolayer structure. If we assume a structural model for the S_{A_1} phase in which the side groups with positional order along the director are packed in a lamellar block constituting the smectic planes [16], the polymer backbone is placed between the lamellae and is able to form a two dimensional

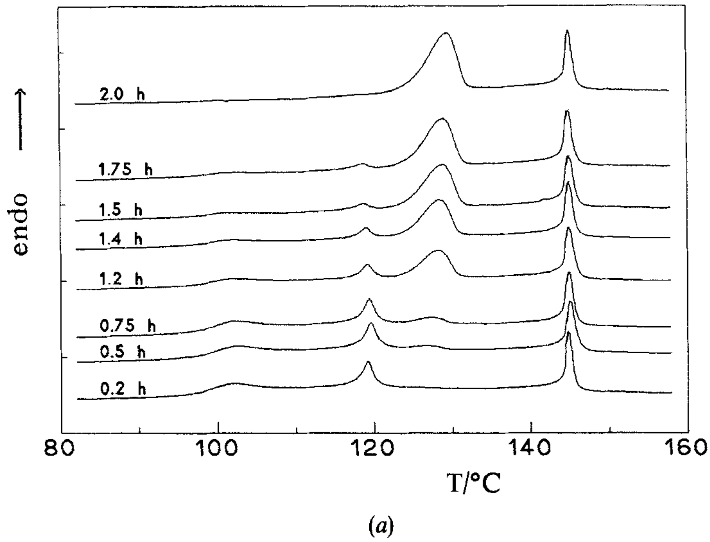

(*a*)

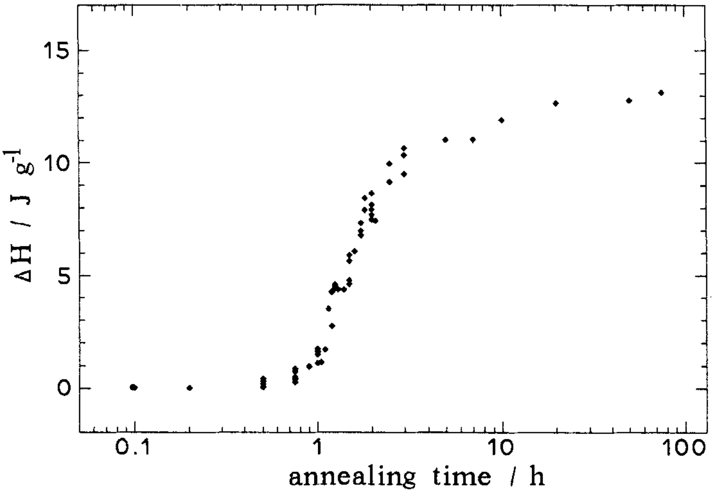

(*b*)

Figure 7. (*a*) DSC traces of polymer $P_{6,4,b}$ depending on annealing time at 115°C. (*b*) Enthalpies of the S_C–N phase transition of polymer $P_{6,4,b}$ depending on annealing time at 115°C.

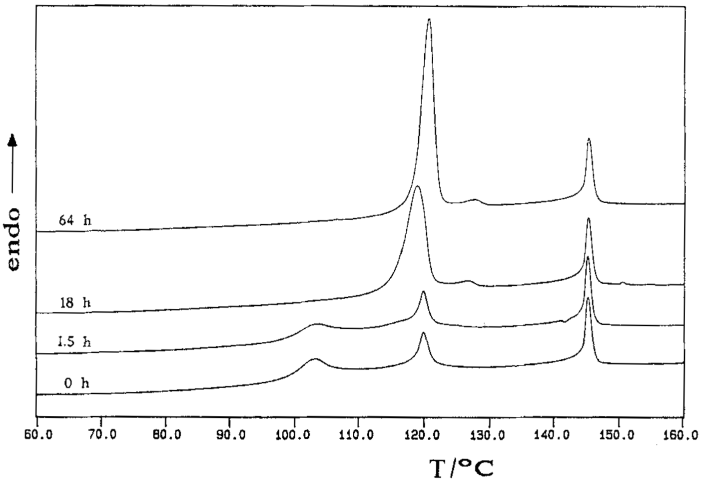

Figure 8. DSC traces of polymer $P_{6,4,b}$ depending on annealing time at 104°C. Both phase transitions from the metastable phase to the unidentified phase X and to the S_{C_2} phase are observed.

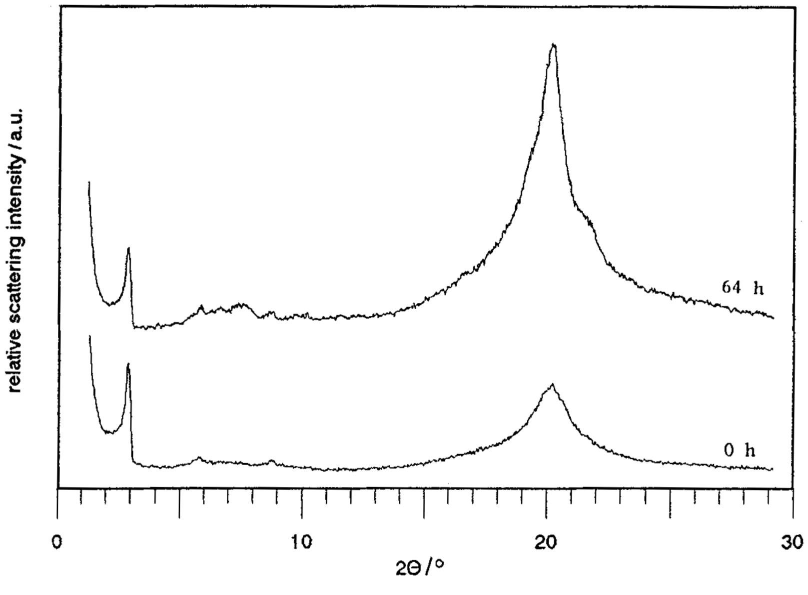

Figure 9. Guinier goniometer curves for the unidentified phase X of polymer $P_{6,4,b}$ depending on annealing time at 103°C.

coil-like structure. We assume that in such a monolayer S_{A_1} structure, the steric hindrance between the spacer of one molecule and the tail of a neighbouring molecule is very high if the length of both the spacer and the tail group is nearly the same.

In order to avoid this steric hindrance, it is necessary that the polymer $P_{6,4}$ is able to form the tilted bilayer S_{C_2} phase on annealing in the S_{A_1} phase at temperatures higher than 104°C. On annealing in this temperature range, we assume that the backbone forms a more ordered structure from which the mesogenic side groups project at an angle near to 90° [17]. The flexible alkyl spacer serves as mediator in achieving this goal. Backbone and mesogenic side groups are then able to form elliptical bodies, which can be moved because there are no or only weak correlations.

At temperatures below 104°C, the mobility of the backbone is too small to achieve the S_{C_2} structure. On annealing, the restricted mobility of the backbone and the mobility of the side groups lead to the unidentified structure assigned as X, which seems to be a crystalline phase. The formation of a packing model depending on annealing is in progress.

References

[1] McArdle, C. B. (editor), 1989, *Side Chain Liquid Crystal Polymers* (Blackie), p. 357 ff.

[2] Ringsdorf, H., and Zentel, R., 1982, *Makromolek. Chem.*, **183**, 1245.

[3] Eich, M., Wendorff, J. H., Ringsdorf, H., and Schmidt, H. W., 1985, *Makromolek. Chem.*, **186**, 2639.

[4] Anderle, K., Birenheide, R., Eich, M., and Wendorff, J., 1989, *Makromolek. Chem. rap. Commun.*, **10**, 477.

[5] Angeloni, A. S., Caretti, D., Carlini, C., Chiellini, E., Galli, G., Altomare, A., Solaro, R., and Laus, M., 1989, *Liq. Crystals*, **4**, 513.

[6] Stumpe, J., Müller, L., Kreysig, D., Hauck, G., Koswig, H., Ruhmann, R., and Rübner, J., 1991, *Makromolek. Chem. rap. Commun.*, **12**, 81.

[7] Angeloni, A. S., Caretti, D., Laus, M., Chiellini, E., and Galli, G., 1991, *J. Polym. Sci. Polym. Chem. Ed.*, **29**, 1865.

[8] Ringsdorf, H., and Schmidt, H. W., 1984, *Makromolek. Chem.*, **185**, 1327.

[9] Eich, M., Wendorff, J. H., Reck, B., and Ringsdorf, H., 1987, *Makromolek. Chem. rap. Commun.*, **8**, 59.

[10] Eich, M., and Wendorff, J. H., 1987, *Makromolek. Chem. rap. Commun.*, **8**, 467.

[11] Seki, T., Tamaki, T., Suzuki, Y., Kawanishi, Y., Ichimura, K., and Aoki, K., 1989, *Macromolecules*, **22**, 3505.

[12] Ortler, R., Bräuchle, C., Miller, A., and Riepl, G., 1989, *Makromolek. Chem. rap. Commun.*, **10**, 189.

[13] Ikeda, T., Horiukchi, S., Karanjit, D. B., Kurihara, S., and Tazuke, S., 1990, *Macromolecules*, **23**, 36.

[14] Ciardelli, F., Carlini, C., Solaro, R., Altomare, A., Pieroni, O., Houben, J. L., and Fissi, A., 1984, *Pure appl. Chem.*, **56**, 329.

[15] Wolff, D., Cackovic, H., and Springer, J., 1991, *Berliner Polymerentage.*

[16] Strzelecki, L., and Liebert, L., 1973, *Bull. Chim. fr.*, 597.

[17] Zugenmaier, P., and Mügge, J., 1984, *Makromolek. Chem. rap. Commun.*, **5**, 11.